Freeze-fracture of neurons in nucleus magnocellularis of the chick

Douglas E. Mattox [1], David R. Olmos [1] and Edwin W. Rubel [2]

[1] *Division of Otolaryngology, University of Texas Health Science Center at San Antonio, San Antonio, TX 78284; and* [2] *Departments of Otolaryngology and Physiology, and Neuroscience Program, University of Virginia School of Medicine, Charlottesville, VA 22908, U.S.A.*

4- to 8-day-old chicks were used to examine the ultrastructure of end bulbs and neurons of nucleus magnocellularis by freeze-fracture and thin section techniques. Both normal animals and animals deafferented by removal of the basilar papilla were used to describe the pre- and postsynaptic membranes of these neurons. Postsynaptic membrane specializations similar to those described in rodents were found in normal and deafferented chicks. In the presynaptic end bulb there was an immediate cessation of endocytotic vesicle formation after deafferentation. There was also a shift in the preferential fracture plane from the presynaptic to postsynaptic membranes 48–72 h after basilar papilla removal. These results indicate that the ultrastructure of this synaptic complex is comparable to that seen in mammals.

freeze-fracture, nucleus magnocellularis, chick, deafferentation

Introduction

Afferent fibers from the avian basilar papilla terminate in two brainstem nuclei: nucleus magnocellularis and nucleus angularis [2]. N. magnocellularis is composed of a homogeneous population of large spherical neurons which receive a dominant excitatory projection from the ipsilateral basilar papilla [2,25]. The organization and ultrastructure of these cells are very similar to the spherical cells of the anteroventral cochlear nucleus (AVCN) of mammals [1,14,26,29]. The primary auditory afferent neurons in both mammals and birds form large calyceal endings (end bulbs of Held) on the cell body of the spherical cells [2,24,30,32]. The pre- and postsynaptic membranes of these large axosomatic contacts are ideal for study with the freeze-fracture technique.

In mammals the axosomatic contact between the afferent end bulb and the spherical cells has multiple small synaptic active zones [7,10,12,19]. The presynaptic membrane has small membrane deformations at these active zones which are presumed to be sites of exocytotic transmitter release. The external leaflet (E-face) of the spherical cell membrane at the active zone has an aggregate of particles (junctional aggregate) which is co-extensive with the presynaptic active zone. It has been suggested that these particles may represent an integral part of the functional synapse, perhaps a receptor protein within the membrane [8].

The extracellular space between the end bulb and spherical cell is widened between active zones, forming channels surrounding single or small groups of active zones. These extracellular channels often contain astrocytic processes. The E-face of the postsynaptic membrane has irregularly shaped aggregates of particles distributed around the active zones (perisynaptic aggregates) [10]. Perisynaptic aggregates preferentially occur over extracellular channels, particularly those containing glial processes. It has been suggested that the perisynaptic aggregates may be ionic pumps, extrajunctional receptors, enzymes for neurotransmitter degradation, or sites of attachment of

---

Address reprint requests to: Douglas E. Mattox, MD, Department of Otolaryngology – Head and Neck Surgery, Johns Hopkins Hospital, 600 N. Wolfe St., Baltimore, MD 21205, U.S.A.
Address all correspondence to: Edwin W. Rubel, Department of Otolaryngology, Box 430, University of Virginia Medical Center, Charlottesville, VA 22908, U.S.A.

cisterns of endoplasmic reticulum [10]. However, the occurrence of perisynaptic aggregates is inconsistent across species. For example, they are not seen in the AVCN of normal rats and mice, but are found in chinchillas and guinea pigs. Therefore, the function of perisynaptic aggregates remains speculative [22].

In addition to junctional aggregates and perisynaptic aggregates, there are scattered background (nonaggregate) particles on the remainder of the postsynaptic E-face membrane.

Orderly changes occurred on the postsynaptic spherical cell membrane after deafferentation by cochlear ablation in the guinea pig [9]. Between 1 and 2 days after ablation, the number of perisynaptic aggregates surrounding the active zones decreased by 90%, and by 4 days all the perisynaptic aggregates had disappeared. At the same time the number of nonaggregate particles increased. There was also a decrease in the number, but an increase in the size, of the junctional aggregates during this same time period. The total number of junctional particles per unit membrane did not change up to 6 days after deafferentation [9].

Nucleus magnocellularis in the chick auditory system is a particularly useful preparation for studies of the relationship between presynaptic and postsynaptic elements. The similarity between n. magnocellularis neurons and the spherical cells of the mammalian AVCN is noted above. In addition, the elegant studies of Jhaveri and Morest [14] stress the homogeneity of n. magnocellularis neurons in the chick and provide a firm basis for further ultrastructural analyses. Detailed studies have been carried out on the physiological and morphological development of n. magnocellularis [13,15,16,28]. Finally the effects of deafferentation on n. magnocellularis neurons have been described [4,6,20,23,33]. Therefore, the chick auditory system allows comparison of physiological events with the ultrastructure seen in freeze-fracture replicas and thin sections. In this study we describe the morphologic features of the axosomatic contacts in n. magnocellularis of normal hatchling chicks. In addition, chicks deafened by removal of the basilar papilla were examined. This manipulation alters the fracture characteristics of the axosomatic contact and allows observation of membrane elements which cannot be seen in normal animals.

Methods

Thirty-six 4- to 8-day-old hatchling White Leghorn chickens were anesthetized with pentobarbital and perfused through the heart with 3% glutaraldehyde and 2% paraformaldehyde in 0.1 M sodium cacodylate and 20 mM $CaCl_2$, at 39°C. After perfusion the skull was opened and placed in fixative before the brain was dissected.

For freeze-fracture the brain was postfixed for 2 h in cold fixative and 200-μm slices were cut on a vibratome. The nucleus magnocellularis was dissected from both sides of the brain and placed in cold 5% glycerol in 0.1 M cacodylate buffer. The tissue was transferred over a 1 h period through a graded series up to 20% glycerol where it remained for one hour. The tissue was then frozen in a Freon 22 slurry cooled with liquid nitrogen and fractured in a Balzers 301 freeze-fracture unit at −119°C. Platinum–carbon replicas were made with electron beam guns with the replica thickness standardized with a quartz crystal monitor. The replicas were cleaned in cold methanol, Clorox bleach, and distilled water before being picked up on Formvar coated grids.

For thin sections the skull remained in cold fixative for 24 h before dissection. After dissection, 200-μm slices were cut through the brain stem and the nucleus magnocellularis was dissected from both sides. The tissue was postfixed at 4°C in 1.5% potassium ferrocyanide and 1% OsO_4 in 0.05 M sodium cacodylate buffer. All slices were dehydrated in a graded series of methanol and embedded in Spurs resin. Sections 1–2 μm thick from each block were examined for orientation before thin sections were cut and stained with uranyl acetate and lead citrate. Thin sections and freeze-fracture replicas were examined with a Siemens 1A electron microscope.

Bilateral basilar papilla removal was performed under light pentobarbital anesthesia. The external auditory meatus was enlarged and the tympanic membrane and columella removed. The membranous basilar papilla was grasped with a small forceps and removed in toto. The basilar papilla was floated in saline and examined for completeness. The animals were allowed to recover from anesthesia and given food and water ad libitum.

The freeze-fracture technique reveals the inter-

nal structure of the lipid bilayer cell membrane [31]. The true external surface and the surface facing the cytoplasm are not seen. 'P-face' refers to the internal surface of the membrane leaflet closest to the cytoplasm and 'E-face' refers to the internal surface of the external membrane leaflet. All micrographs are shown with the platinum shadowing coming from the bottom of the micrograph.

Results

Normal animals

Axosomatic contact. Large axosomatic contacts between the afferent end bulb and the n. magnocellularis neuron were easily identified in both thin sections and freeze-fracture replicas (Fig. 1). Features of this contact included: multiple synaptic active zones, presynaptic vesicles within the end bulb near the active zones (Figs. 1, 6), and postsynaptic densities in the n. magnocellularis neuron cytoplasm adjacent to the active zones (Fig. 6). There were extracellular channels between the end bulb and the n. magnocellularis neuron surrounding the active zones, which frequently contained glial processes (Figs. 1, 12). In normal animals the plane of cleavage produced by the freeze-fracture technique was along the presynaptic membrane at the active zone, but followed the postsynaptic membrane between the active zones (Fig. 7). This relationship was reversed in the deafferented animals (Fig. 9).

In addition to the primary afferent end bulbs, bouton-shaped terminals could also be identified in both thin-section and freeze-fracture replicas (Fig. 3). These terminals were packed with synaptic vesicles throughout the terminal and did not have discrete active zones that we could identify. These endings appear comparable to the non-primary endings described by Parks [24] and Hackett et al. [11].

Active zones. In thin-sections the membrane at the end bulb active zone has a slight curvature with the convex side toward the end bulb (Fig. 6). Cross-fractures of the active zone in freeze-fracture replicas show a similar bulging of the active zone into the end bulb (Figs. 1, 7). The active zone

on the presynaptic P-face of the end bulb may also be identified by a collection of particles which are larger than the background particles (Fig. 7).

The description of the active zone in normal chicks is limited to the presynaptic membranes, because the fracture plane did not fall along the postsynaptic membrane at the active zone. As in mammals presynaptic membrane specializations associated with active zones could only be seen in deafferented animals. These specializations are described in the section on deafferented animals below.

Perisynaptic aggregates. The postsynaptic E-face membrane had irregularly-shaped aggregates of loosely-packed, heterogeneously-sized particles scattered around the active zones. These perisynaptic aggregates were regularly observed in both normal (Figs. 12, 14) and deafferented chickens (Figs. 8, 11). These aggregates were not associated with presynaptic specializations, but were found overlying the extracellular channels between active zones (Figs. 12, 14). Additional fragments of P-face membrane were found attached to the postsynaptic E-face at the site of the perisynaptic aggregates (Figs. 12, 14). In cross-fractures of the n. magnocellularis neuron cytoplasm, these membrane fragments were continuous with subsurface cisterns (Figs. 12, 14).

In addition to their location over extracellular spaces around active zones, these aggregates were also found associated with larger expanses of astrocytic membrane adjacent to the n. magnocellularis neurons [5].

Background particles. The postsynaptic P-face membrane had a high concentration of background particles typical of P-face membrane. The density of background particles on the postsynaptic E-face membrane, exclusive of particle aggregates, averaged $92/\mu m^2$.

End bulb endocytotic vesicles. The extracellular channels between the pre- and postsynaptic membranes produced shallow grooves in the presynaptic membrane. In normal animals there were many pinocytic vesicle sites in the presynaptic membrane along these grooves (Fig. 17).
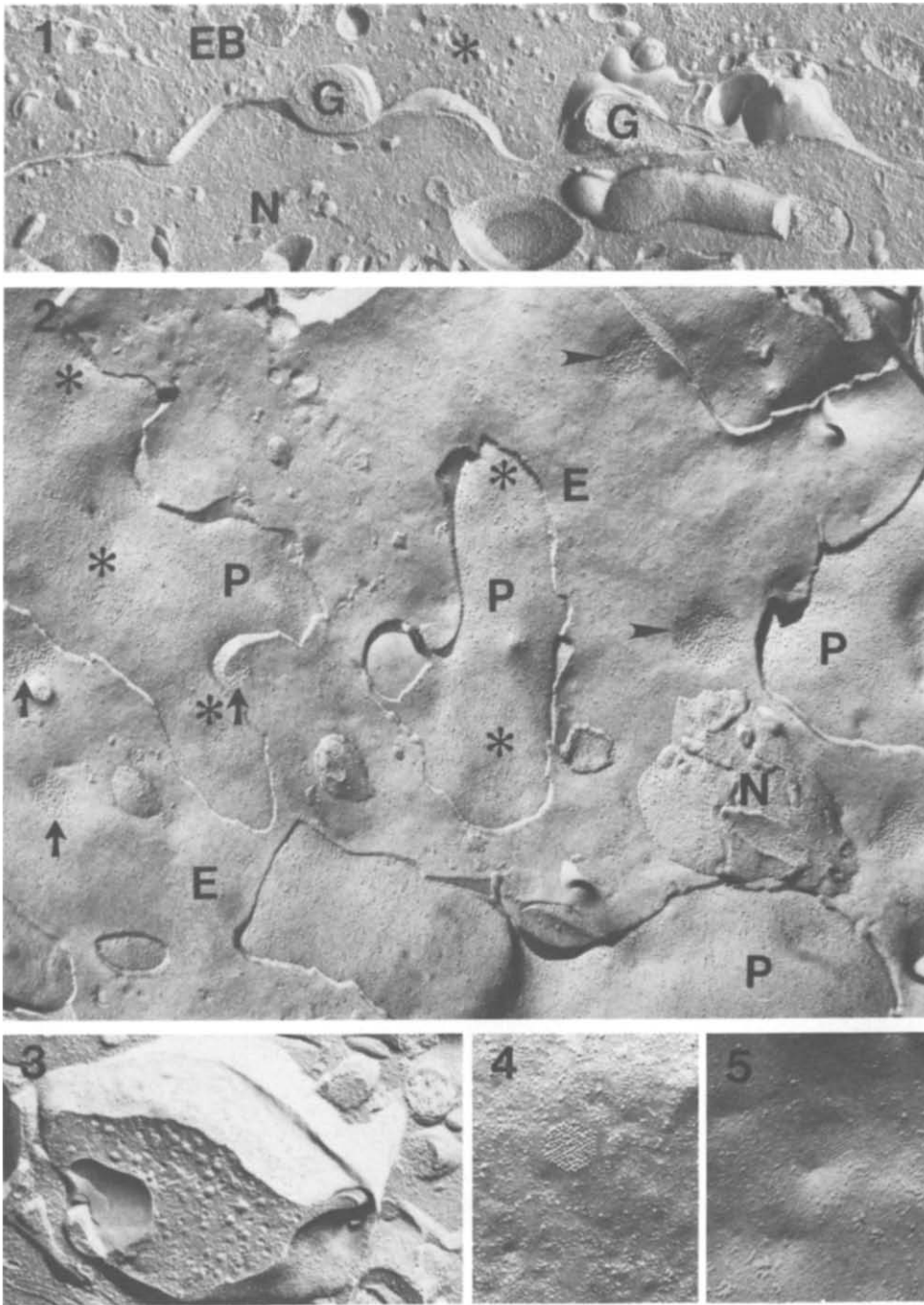
70

Fig. 1. A freeze-fracture replica from a control animal showing a cross-fractured axosomatic contact between a primary afferent end bulb (EB) and a n. magnocellularis neuron (N) in chick nucleus magnocellularis. The end bulb has an active zone (∗) with the n. magnocellularis neuron indicated by the collection of presynaptic vesicles adjacent to a convexity in the membranes. Adjacent to the active zone is an enlarged extracellular space containing glial processes (G) (×33000). Platinum shadowing is from the bottom of the micrograph in this and all subsequent freeze-fracture micrographs.

Fig. 2. A freeze-fracture replica showing the axosomatic contact between end bulb and n. magnocellularis neuron in a chick 12 h after removal of the basilar papilla. The membranes are seen from the perspective from within the postsynaptic neuron. The E-face of the

Deafferented animals

Active zones. In normal animals the fracture plane followed the presynaptic membrane at the active zone and the postsynaptic membrane between active zones. By 12 h after deafferentation, the fracture plane shifted, such that fragments of the postsynaptic membranes could be seen at some of the active zones. The E-face membrane at the active zone had aggregates of large, homogeneously-sized, densely-packed particles (Figs. 2, 8). Replicas showing the P-face presynaptic membrane adjacent to these densely-packed aggregates had a shallow depression in the membrane and scattered large particles characteristic of active zones (Fig. 9). Fractures showing cross-fractured presynaptic cytoplasm adjacent to these aggregates showed collections of presynaptic vesicles.

In the 72-h and 6-day deafferented animals, the fracture plane tended to follow the postsynaptic membrane and substantially more postsynaptic membrane specializations could be seen. Numerous junctional aggregates could be seen on these expanses of E-face membrane. These junctional aggregates had an average diameter of 0.3 μm. This is comparable to the maximum length of synaptic specializations seen in thin sections (see also [24]).

The postsynaptic P-face membrane at the active zone at these time periods was characterized by a slight elevation, 0.3 μm in diameter, with numerous pits over its surface (Fig. 10).

Perisynaptic aggregates. Perisynaptic aggregates were found on all postsynaptic E-face membranes at all time periods examined, including 6-day deafferented animals. In fractures where both perisynaptic and junctional aggregates were present, subsurface cistern membranes were associated only with the perisynaptic aggregates (Figs. 15, 16).

End bulb endocytotic vesicles. No endocytotic vesicle sites could be identified in the end bulb membranes after removal of the basilar papilla (compare Figs. 17 and 18), even in animals which were fixed immediately after basilar papilla removal.

Background particles. The density of background particles on the E-face membrane increased after deafferentation to 188/μm^2 at 72 h. At 6 days after deafferentation the membranes showed moderate degeneration, and particle counts could not be done reliably.

Gap junctions. Gap junctions were found on the P-face of both end bulb membrane (Fig. 4) and n. magnocellularis neuron membranes (Fig. 5). The frequency of gap junctions was not great enough to quantitate; however, it was common to find one or two gap junctions when 10 μm^2 of membrane was exposed. Gap junctions have also been seen in rat and mouse AVCN [22].

---

postsynaptic membrane (E) has several windows through which the P-face (P) of the presynaptic membrane of the end bulb may be seen. Active zones on the end bulb (* above) are seen as slight depressions with a collection of particles larger than the background particles. The active zones on the postsynaptic E-face membrane (arrowhead) have densely-packed particle aggregates lying in shallow depressions in the membrane. Other membrane specializations (perisynaptic aggregates) are evident on the n. magnocellularis neuron E-face membranes (arrows). These aggregates have heterogeneously-sized particles and irregular borders (perisynaptic aggregates). There is a small amount of cross-fractured n. magnocellularis cytoplasm overlying the E-face membrane (N) ($\times$30000).

Fig. 3. A cross-fracture of a non-primary afferent from a control animal. Features which distinguish this terminal from primary afferent terminals include its boutonal shape and a wider distribution and denser packing of presynaptic vesicles throughout the terminal. The terminal also lacks a discrete active zone typically seen in primary afferent terminals ($\times$33000).

Fig. 4. A gap junction is shown on this presynaptic P-face membrane as a hexagonally packed collection of particles (24 h deafferented chick, $\times$65000).

Fig. 5. A gap junction on the postsynaptic P-face membrane is seen as a hexagonally packed collection of pits (24 h deafferented chick, $\times$65000).
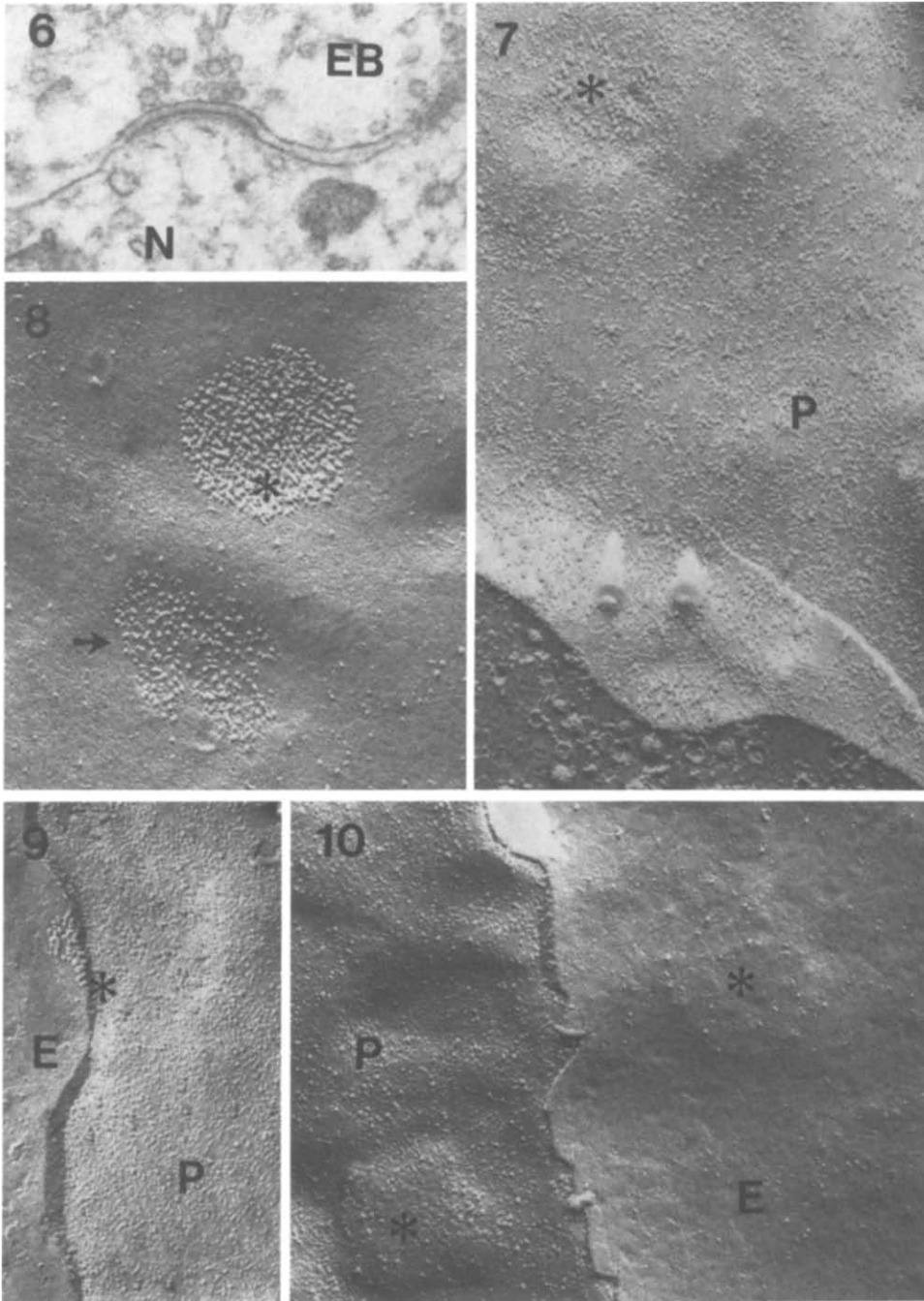
Fig. 6. A thin section of a synaptic contact between an end bulb (EB) and n. magnocellularis neuron (N) from a control animal. Note the direction of curvature of the membranes at the active zone, presynaptic vesicles and postsynaptic density ($\times 60\,000$).

Fig. 7. A freeze-fracture replica of an end bulb from a control animal. This micrograph is oriented upside down relative to Fig. 6 because of the angle of platinum shadowing. The micrograph shows cross-fractured cytoplasm containing presynaptic vesicles in the lower half of the frame, and P-face membrane above (P). The P-face membrane has a slight depression at the active zone and an accumulation of particles which are slightly larger than the background particles. A second active zone (*) on the P-face membrane is seen in the upper left-hand side of the micrograph ($\times 60\,000$).

73

Discussion

The general morphology of the neurons of nucleus magnocellularis is similar to the spherical cells of AVCN of the guinea pig, cat and chinchilla [1,2,14,26,29]. In all species the primary afferent fibers have large calyceal endings which have broad axosomatic contacts with the spherical cell. These end bulbs have multiple synaptic active zones with the soma of the spherical cell [7,10,12,19,30].

In the chick membrane specializations at the active zone revealed by the freeze-fracture technique are similar to those seen in the other species not above. On the postsynaptic E-face membrane, active zones are characterized by aggregates of large, homogeneously-sized particles. These aggregates have smooth circular borders and lie on shallow concavities of the membrane when viewed from the perspective of within the n. magnocellularis neuron. Cross-fractures through the presynaptic cytoplasm adjacent to these aggregates show collections of presynaptic vesicles similar to the presynaptic concentration of vesicles seen in thin sections. E-face junctional aggregates have been associated with putative glutamatergic excitatory synapses, including those of the mammalian central nervous system [17,18] and arthropod neuromuscular junction [27]. It has been suggested that these particles may represent an integral part of the functional synapse, perhaps a receptor protein within the membrane [8].

On the postsynaptic P-face membrane elevations with small deformations (pits) could be identified. Pits on a membrane surface are produced by particles on the complementary membrane leaflet. We interpret these structures as corresponding to the E-face junctional aggregates. Similar but slightly smaller regions on the spherical cell cytoplasmic leaflet were identified in guinea pig AVCN [10]. However, on the basis of a difference in size and an association with enlarged extracellular spaces, these regions were thought to correspond to perisynaptic aggregates rather than active zones [10]. We do not find a size discrepancy between the P-face specializations and junctional aggregates; both averaged 0.3 μm in diameter. In the chick n. magnocellularis the spatial distribution of these structures over the neuronal cell membrane corresponds to active zones rather than perisynaptic aggregates. Lastly, the perimeter of these P-face specializations was circular, whereas perisynaptic aggregates have irregular borders. The observation that the particles of junctional aggregates interact with both membrane leaflets of the postsynaptic cell suggests that these particles may be synaptic receptor proteins [8].

The aggregates of heterogeneously-sized particles with irregular perimeters resemble the perisynaptic aggregates described by Gulley et al. [10]. These aggregates have been found on the E-face of cells associated with end bulbs of Held, including the AVCN of the cat, chinchilla and guinea pig, and the medial nucleus of the trapezoid body in the guinea pig. These aggregates are absent in the AVCN of normal rats and mice. In the chick, cross-fractures show that these aggregates fall over extracellular channels between synaptic active zones and that these channels frequently contain

Fig. 8. The E-face of the n. magnocellularis neuron 3 days after deafferentation showing two different specializations. A junctional aggregate (active zone) (*) is shown with densely-packed large particles. There is also a perisynaptic aggregate (arrow) which has heterogeneously-sized particles, irregular borders, and lower particle density ($\times 60000$).

Fig. 9. A freeze-fracture replica of a 24 h deafferented animal showing fragments of presynaptic P-face (P) and postsynaptic n. magnocellularis E-face (E) across a single active zone. The presynaptic membrane shows a slight depression and a few large particles. The postsynaptic E-face shows a fragment of a densely-packed particle aggregate. In normal animals the fracture plane tended to follow the presynaptic membrane at the active zone and full extent of the junctional aggregates was never seen, whereas in deafferented animals the full extent of these aggregates could be seen (see Fig. 8) ($\times 60000$).

Fig. 10. A freeze-fracture replica of an axosomatic contact seen from the perspective from within the end bulb in a 6-day deafferented animal. The end bulb E-face membrane (E) occupies the right side of the micrograph and the P-face postsynaptic membrane (P) the left. Elevations can be seen in both membranes corresponding to dome-shaped active zones (*). Small pits can be seen at the active zone in the postsynaptic P-face membrane which correspond to the impressions left by the E-face junctional particles ($\times 60000$).
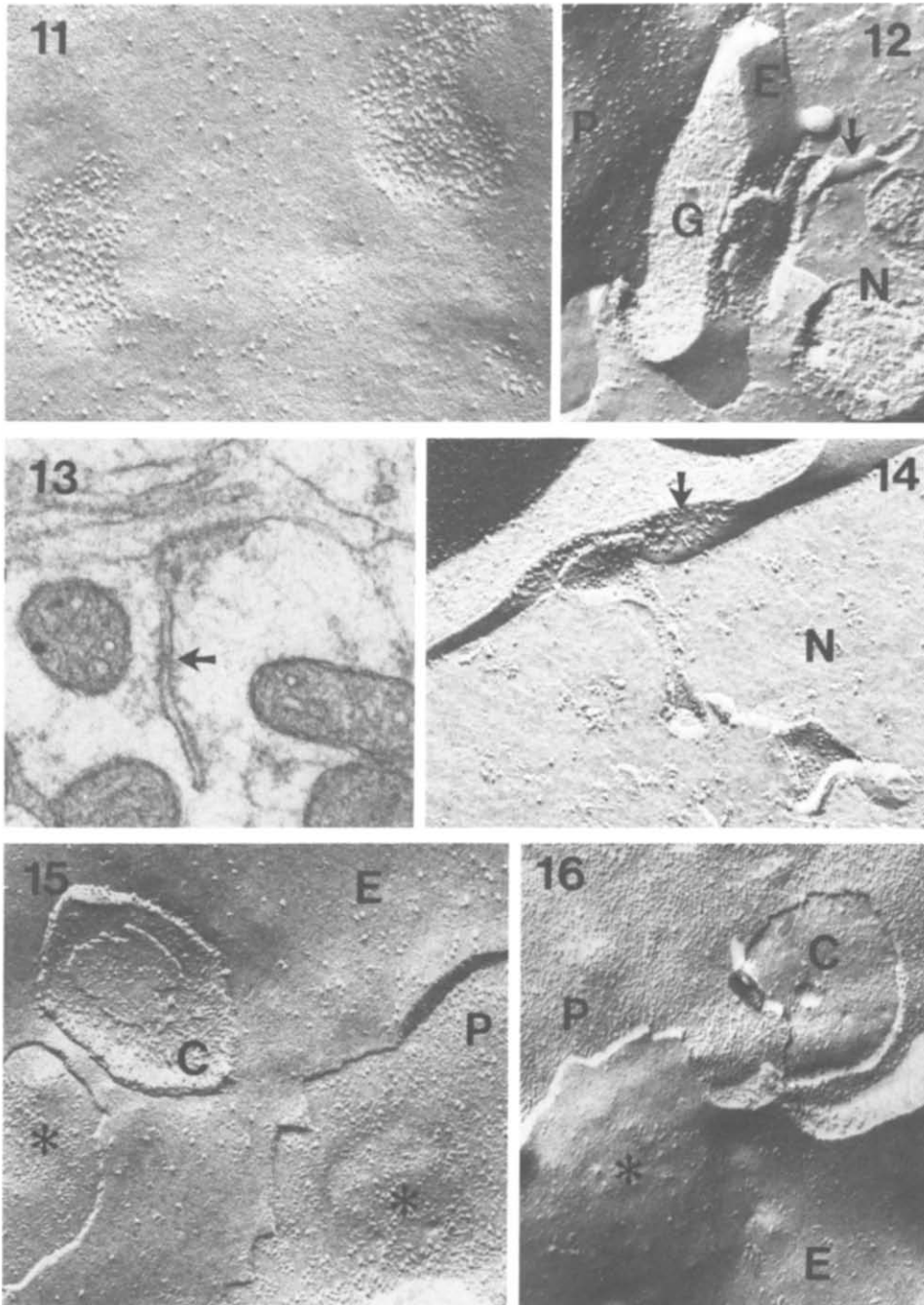
Fig. 11. In this 72-h deafferented animal the E-face n. magnocellularis neuron membrane (N) has several aggregates of heterogeneously-sized particles. These aggregates have irregular perimeters and are found between active zones and over extracellular channels (see Figs. 12, 14) (×60000).

Fig. 12. A cross-fracture showing n. magnocellularis neuron cytoplasm at the right (N) and end bulb P-face membrane at the left (P) in a control animal. There is a glial process (G) intercalated between the two cells. The exposed postsynaptic E-face membrane (E) has a particle aggregate which is in turn partially covered with membrane which is in continuity with cytoplasmic endoplasmic reticulum (arrow) (×60000).

glial processes. As in chinchilla and guinea pig, these aggregates were also found in association with large astrocytic membranes abutting against the spherical cell [10]. The distribution of the perisynaptic aggregates in the chick is more irregular than the roughly geometric distribution around active zones seen in chinchilla and guinea pig.

The association of the perisynaptic aggregates and subsurface cisterns in the spherical cell cytoplasm has been described in the guinea pig. However, both structures were also found independently of each other. Therefore, it was concluded that when they were found in juxtaposition it was fortuitous [10]. In the chick, fragments of the subsurface cisterns were very common on E-face membranes and were always associated with particle aggregates. Cross-fractures of n. magnocellularis neuron cytoplasm adjacent to perisynaptic aggregates always demonstrated a subsurface cistern. The functional significance of this association is not understood. However, it does provide a possible route for communication between the extracellular space and the internal structures of the neuron. These perisynaptic aggregates cannot be interpreted as absolute requirements for the function or attachment of subsurface cisterns because rat and mouse have many cisterns without perisynaptic aggregates [22].

Perisynaptic aggregates in the chick also exhibited different behavior after deafferentation than in the guinea pig. In guinea pig perisynaptic aggregates were no longer identifiable two days after deafferentation [9]. However, in the chick they were still present up to six days after deafferentation. We can supply no compelling hypothesis for these species differences, particularly since the postsynaptic reaction of n. magnocellularis neurons to deafferentation is essentially complete within 2–5 days after basilar papilla removal [4,6]. It may be interesting to note, however, that removal of the basilar papilla in the chick results in progressive loss of ganglion cells. Approximately 70% remain 4 days after cochlear removal [4]. In mammals, on the other hand, the modiolus and spiral ganglion cells are usually destroyed in the process of cochlear removal.

A number of changes did occur in the end bulb and n. magnocellularis neurons in response to basilar papilla removal. The earliest change was the disappearance of coated vesicle sites from the end bulb. In the normal animal coated vesicles can be seen in the end bulb membrane along the extracellular channels. These sites were absent in all deafferented animals, even when animals were perfused immediately after cochlear removal. This result suggests that endocytotic activity is coupled to the activity of neurons. In this regard, it is interesting to note that the extracellularly recorded impulse activity in n. magnocellularis completely disappears immediately when the basillar papilla is removed [3].

As in the guinea pig, there was an increase in the density of background particles on the postsynaptic E-face membrane after basilar papilla

Fig. 13. A thin section from a control animal of an area similar to Figs. 12 and 14. There is a n. magnocellularis neuron with a subsurface cistern in continuity with endoplasmic reticulum (arrow). This structure is not associated with a synaptic active zone (×60000).

Fig. 14. A cross-fracture showing E-face membrane and the adjacent n. magnocellularis neuron cytoplasm (N) in a control animal. A perisynaptic aggregate (arrow) is partially covered by a fragment of subsurface cistern membrane (×60000).

Fig. 15. An external leaflet (E-face) of the n. magnocellularis neuron membrane (E) as seen from the perspective from within the end bulb in a 48-h deafferented animal. There is a large fragment of subsurface cistern membrane (C) attached to the E-face membrane. The subsurface cistern membrane also has an additional fragment of E-face membrane attached to it produced when the fracture jumped across the cistern to its innermost lamina. At the lower right there is exposed presynaptic P-face (P) with an active zone (∗) (×60000).

Fig. 16. A freeze-fracture replica from a 24-h deafferented animal seen from the perspective from within the bulb. This view represents the complement of Fig. 12. The postsynaptic P-face membrane (P) has a window exposing another membrane immediately beneath it (C). This membrane is the E-face of a subsurface cistern. In the lower left is an active zone (∗) on the end bulb E-face (E) (×60000).
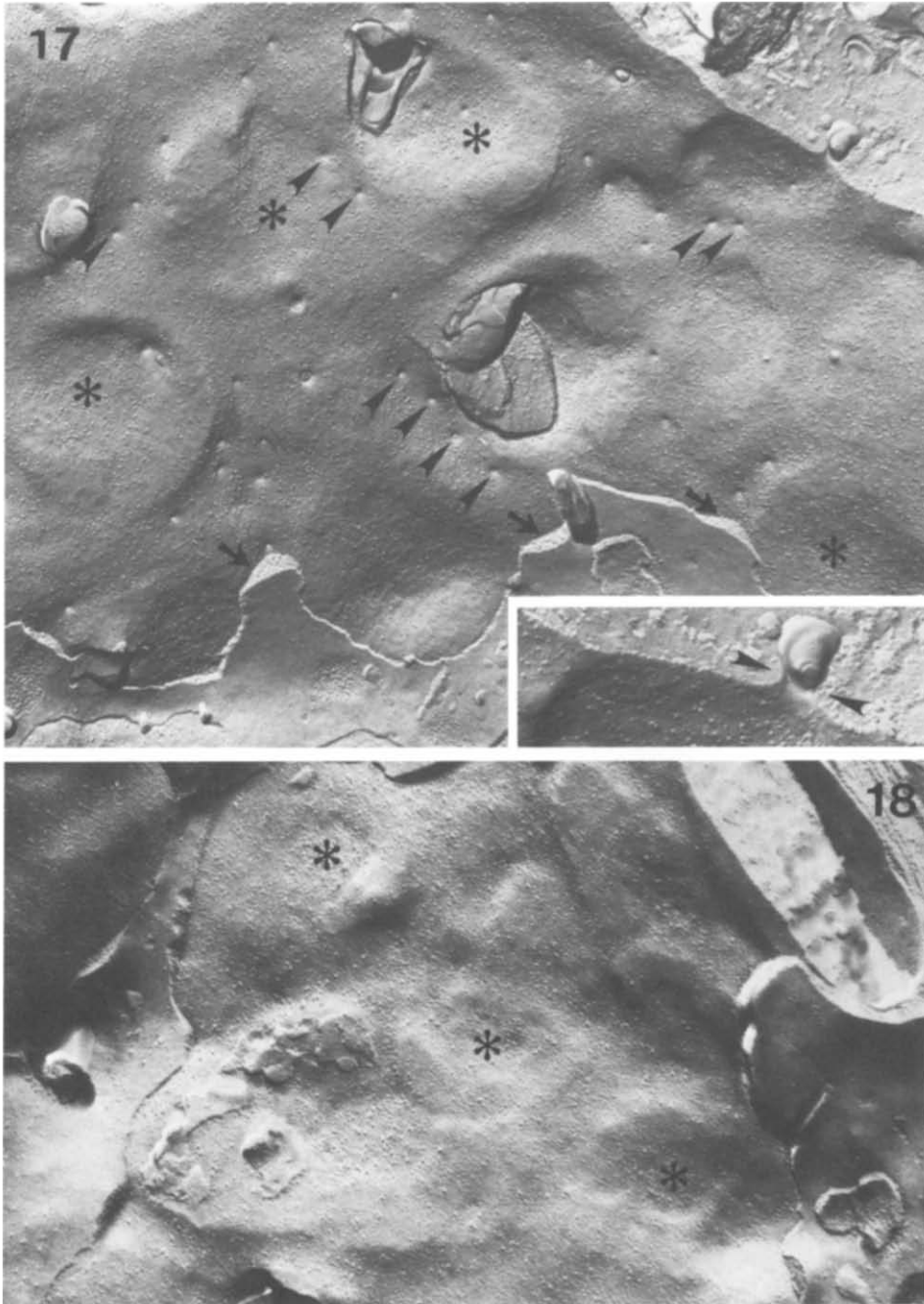
Fig. 17. A large expanse of control animal end bulb P-face showing multiple active zones (*) separated by shallow grooves produced by extracellular channels. The thickness of these extracellular channels can be seen where it is cross-fractured (arrows). Numerous endocytotic vesicle fusion sites are seen along these channels (arrowheads) (×35000). In the inset a cross-fracture of one of these endocytotic sites shows invagination of the cell membrane into the end bulb cytoplasm (arrowheads) (×60000).

Fig. 18. A view similar to Fig. 17 of an end bulb P-face 3 days after deafferentation. Shallow grooves in the end bulb from extracellular channels and active zones (*) are still identifiable; however, there are no endocytotic vesicle fusion sites along the extracellular channels (×35000).

removal; however, this occurred without a concomitant decrease in perisynaptic aggregates as described in the guinea pig [9].

In all species examined there is a difference in the preferential plane of fracture between normal and deafferented animals. In normal animals the plane of fracture preferentially occurs through the presynaptic membranes at the active zone. Thus, nothing more than an occasional fragment of postsynaptic specialization is seen in normal animals. The shift of the fracture plane after deafferentation to the postsynaptic membrane allows the full characterization of the postsynaptic specializations [9]. Early in development, before the onset of behavioral responses or vertex recorded evoked potentials, the preferential plane of fracture is similar to that found in deafferented animals. At approximately the time when responses to sound are first recorded, the fracture plane shifts to the presynaptic membrane [21]. The reasons for the changes in the fracture plane during maturation and following deafferentation are unknown, although they both temporally correspond with changes in ongoing synaptic efficacy. It will be of interest to relate these changes to alterations of the biochemical and functional status of the synapse.

More important than the differences is the consistency of the morphology and ultrastructure of the first central auditory system synapse among these widely divergent species. This consistency of ultrastructure further substantiates the chick as a valuable model for study of auditory function.

Acknowledgements

References

1 Boord, R.L. (1969): The anatomy of the avian auditory system. Ann. N.Y. Acad. Sci. 167, 186–198.

2 Boord, R.L. and Rasmussen, G.L. (1963): Projection of the cochlear and lagenar nerves on the cochlear nuclei of the pigeon. J. Comp. Neurol. 120, 463–475.

3 Born, D.E. and Rubel, E.W. (1984): Cochlear removal eliminates physical activity in brain stem auditory nuclei of the chicken. Neurosci. Abstr. 10, 843.

4 Born, D.E. and Rubel, E.W. (1985): Afferent influences on brainstem auditory nuclei of the chicken: Neuron number and size following cochlea removal. J. Comp. Neurol. (in press).

5 Dermeitzel, R. (1974): Junctions in the central nervous systems of the cat. III. Gap junctions and membrane-associated orthogonal particle complexes (MOPC) in astrocytic membranes. Cell Tiss. Res. 149, 121–135.

6 Durham, D. and Rubel, E.B. (1985): Afferent influences on brainstem auditory nuclei of the chicken: Changes in succinate dehydrogenase activity following cochlea removal. J. Comp. Neurol. (in press).

7 Gentshev, T. and Sotelo, C. (1973): Degenerative patterns in the ventral cochlear nucleus of the rat after primary deafferentation: An ultrastructural study. Brain Res. 62, 37–60.

8 Gulley, R.L. (1979): The freeze-fracture technique as a tool in neurobiology. Trends Neurosci. 2, 237–240.

9 Gulley, R.L., Wenthold, R.J. and Neises, G.R. (1977): Remodeling of neuronal membranes as an early response to deafferentation: A freeze-fracture study. J. Cell Biol. 75, 837–850.

10 Gulley, R.L., Landis, D.M.D. and Reese, T.S. (1978): Internal organization of the membranes at end bulbs of Held in the anteroventral cochlea nucleus. J. Comp. Neurol. 180, 707–742.

11 Hackett, J.T., Jackson, H. and Rubel, E.W. (1982): Synaptic excitation of the second and third order auditory neurons in the avian brain stem. Neuroscience 7, 1455–1469.

12 Ibata, Y. and Pappas, G.D. (1976): The fine structure of synapses in relation to large spherical neurons in the anterior ventral cochlear nucleus of the cat. Neurocytology 5, 395–406.

13 Jackson, H., Hackett, J.T. and Rubel, E.W. (1982): Organization and development of brain stem auditory nuclei in the chick: Ontogeny of postsynaptic responses. J. Comp. Neurol. 210, 80–86.

14 Jhaveri, S. and Morest, D.K. (1982): Neuronal architecture in nucleus magnocellularis of the chicken auditory system with observations on nucleus laminaris: a light and electron microscope study. Neuroscience 7, 809–836.

15 Jhaveri, S. and Morest, D.K. (1982): Sequential alterations of neuronal architecture in nucleus magnocellularis of the developing chicken: a Golgi study. Neuroscience 7, 837–853.

16 Jhaveri, S. and Morest, D.K. (1982): Sequential alterations of neuronal architecture in nucleus magnocellularis of the developing chicken: an electron microscope study. Neuroscience 7, 855–870.

17 Landis, D.M. and Reese, T.S. (1974): Differences in membrane structure between excitatory and inhibitory synapses in the cerebellar cortex. J. Comp. Neurol. 155, 93–126.

18 Landis, D.M.D., Reese, T.S. and Raviola, E. (1974): Differences in membrane structure between excitatory and inhibitory components in the reciprocal synapse in the olfactory bulb. J. Comp. Neurol. 155, 67–92.

19 Lenn, N.J. and Reese, T.S. (1966): The fine structure of nerve endings in the nucleus of the trapezoid body and the ventral cochlear nucleus. Am. J. Anat. 118, 375–390.

20 Levi-Montalcini, R. (1949): The development of the

acoustico-vestibular centers in the chick embryo in the absence of the afferent root fibers of the descending fiber tracts. J. Comp. Neurol. 91, 209–241.

21 Mattox, D.E., Neises, G.R. and Gulley, R.L. (1982): A freeze-fracture study of the maturation of synapses in the anteroventral cochlear nucleus of the developing rat. Anat. Rec. 204, 281–287.

22 Mattox, D.E., Neises, G.R. and Gulley, R.L. (1983): Species differences in the synaptic membranes of the end bulb of Held revealed with the freeze-fracture technique. Anat. Rec. 205, 57–63.

23 Parks, T.N. (1979): Afferent influences on the development of the brainstem auditory nuclei of the chicken: otocyst ablation. J. Comp. Neurol. 183, 665–678.

24 Parks, T.N. (1981): Morphology of axosomatic endings in the avian cochlear nucleus: Nucleus magnocellularis of the chicken. J. Comp. Neurol. 203, 425–440.

25 Parks, T.N. and Rubel, E.W. (1978): Organization and development of the brain stem auditory nuclei of the chicken: Primary afferent projections. J. Comp. Neurol. 180, 439–448.

26 Ramón y Cajal, S. (1908): Les ganglions terminaux du nerf acoustique des oiseaux. Frab. Inst. Cajal. Invest. Biol. 6, 195–225.

27 Rheuben, M.B. and Reese, T.S. (1978): Three dimensional structure and membrane specifications of moth excitatory neuromuscular synapse. J. Ultrastruct. Res. 65, 95–111.

28 Rubel, E.W., Smith, D.J. and Miller, J.C. (1976): Organization and development of brain stem auditory nuclei of the chicken: Ontogeny of N. magnocellularis and N. laminaris. J. Comp. Neurol. 166, 469–490.

29 Rubel, E.W. and Parks, T.N. (1975): Organization and development of the brain stem auditory nuclei of the chicken: Tonotopic organization of N. magnocellularis and N. laminaris. J. Comp. Neurol. 164, 411–434.

30 Ryugo, D.K. and Fekete, D.M. (1982): Morphology of primary axosomatic endings in the anteroventral cochlear nucleus of the cat: A study of the endbulbs of Held. J. Comp. Neurol. 210, 239–257.

31 Sandri, C., Van Buren, J.M. and Akert, K. (1982): Membrane Morphology of the Vertebrate Nervous System: A study with Freeze-Etch Technique. Progress in Brain Research, Vol. 46, Elsevier Biomedical Press, Amsterdam.

32 Schwartz, A.M. and Gulley, R.L. (1978): Non-primary afferents to the principal cell in the rostral cochlear nucleus of the guinea pig. A correlative thin section and freeze-fracture study. Am. J. Anat. 153, 489–496.

33 Steward, O. and Rubel, E.W. (1985): Afferent influences on brain stem auditory nuclei of the chicken: Cessation of amino acid incorporation as an antecedent to age-dependent transneuronal degeneration. J. Comp. Neurol. (in press).